

Supporting information

“Carrier-drug” layer-by-layer hybrid assembly of biocompatible polydopamine nanoparticles to amplify photo-chemotherapy

Lingyu Lv^a, Hao Cheng^a, Zhen Wang^a, Zhangyi Miao^a, Feng Zhang^a, Jie Chen^a, Gang Wang^a, Ling Tao^b, Jianping Zhou^a, Huaqing Zhang^{a, *}, Yang Ding^{a, b, *}

^aState Key Laboratory of Natural Medicines, Department of Pharmaceutics, China Pharmaceutical University, Nanjing, 210009, China

^bThe High Efficacy Application of Natural Medicinal Resources Engineering Center of Guizhou Province, School of Pharmaceutical Sciences, Guizhou Medical University, Guiyang 550025, China

* Corresponding authors.

E-mail: Yang Ding, dydszyzf@163.com; Huaqing Zhang, zhanghq0527@163.com.

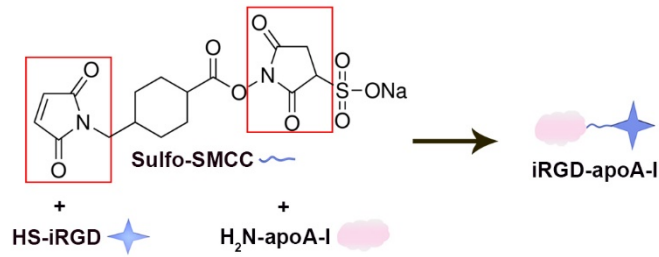


Fig. S1 Synthetic scheme for iRGD-apoA-I.

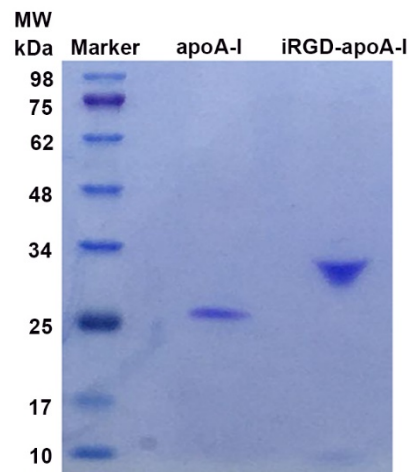


Fig. S2 SDS-PAGE analysis of apoA-I, iRGD-apoA-I, and marker, respectively.

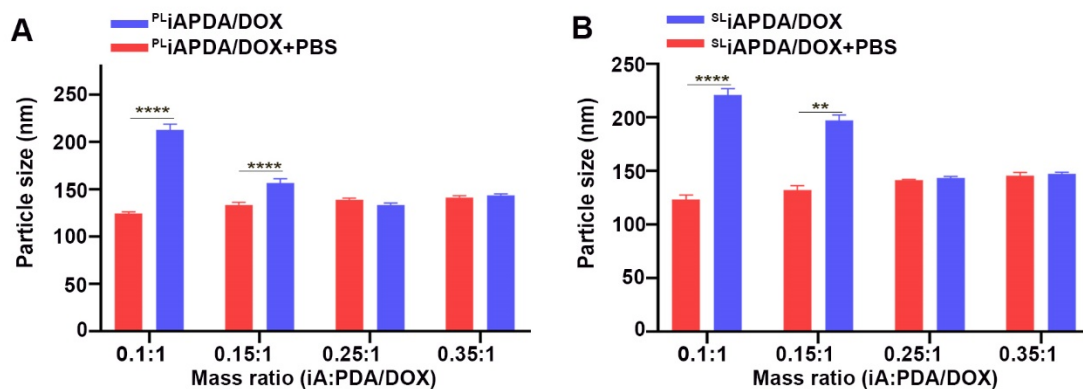


Fig. S3 The size distribution measured by dynamic light scattering of ^{PLi}iAPDA/DOX (A) and ^{SLi}iAPDA/DOX (B) prepared with different iRGD-apoA-I (iA): PDA/DOX mass ratio and incubation with PBS for 24 h. Data were presented as mean \pm SD, $n = 3$. ** $P < 0.01$, **** $P < 0.0001$.

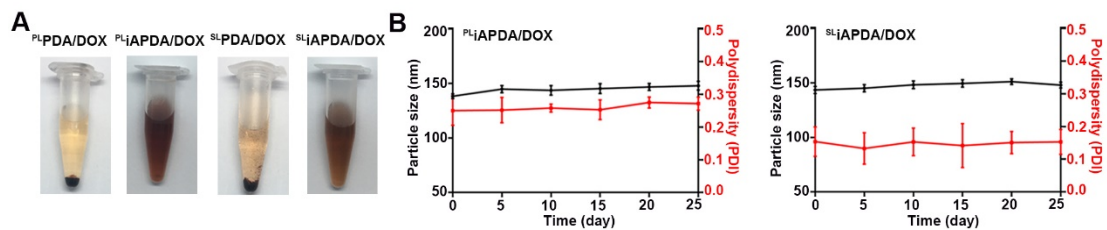


Fig. S4 (A) The stabilization of $^{PL}PDA/DOX$, $^{SL}PDA/DOX$, $^{PLi}APDA/DOX$, and $^{SLi}APDA/DOX$ suspended in PBS after incubation for 24 h. (B) The change in the particle sizes and polydispersity index of $^{PLi}APDA/DOX$ and $^{SLi}APDA/DOX$ during incubation in PBS (pH = 7.4) at 4 °C for 25 days, respectively. Data were presented as mean \pm SD, $n = 3$.

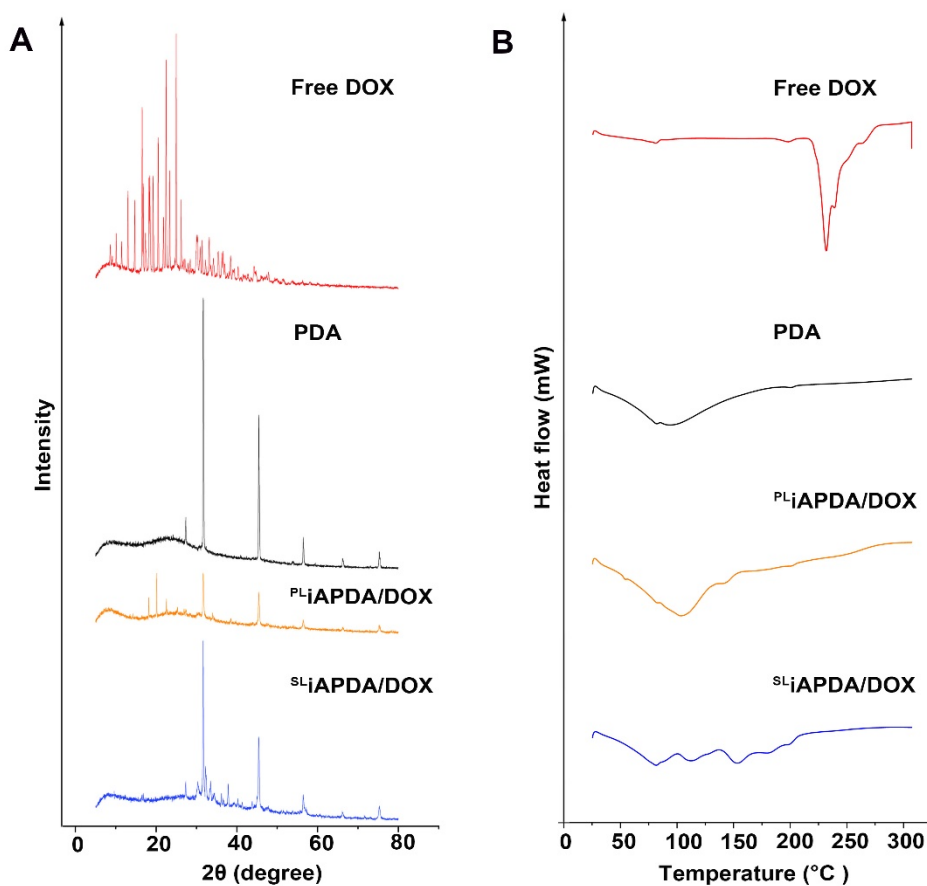


Fig. S5 XRD analysis (A) and DSC thermograms (B) of free DOX, PDA, $^{PLi}APDA/DOX$, and $^{SLi}APDA/DOX$.

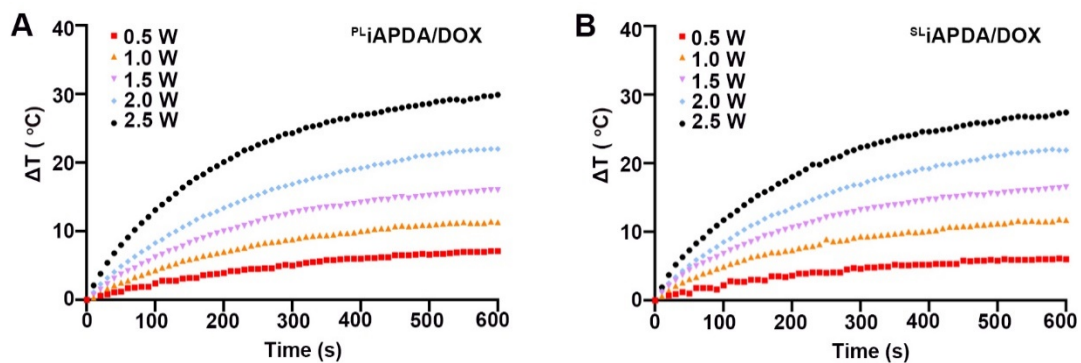


Fig. S6 The photothermal capability of ^{PLi}iAPDA/DOX (A) and ^{SLi}iAPDA/DOX (B) at various NIR laser power (200 $\mu\text{g/mL}$ of PDA), respectively.

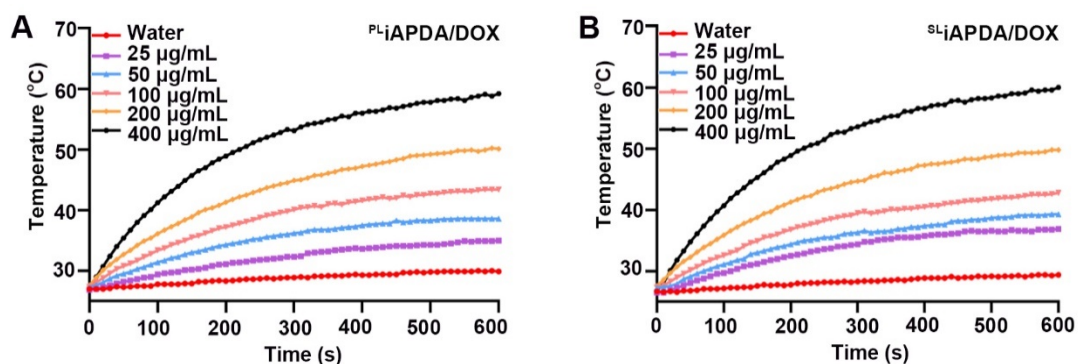


Fig. S7 The photothermal capability of ^{PLi}iAPDA/DOX (A) and ^{SLi}iAPDA/DOX (B) at different PDA concentrations (2 W/cm^2), respectively.

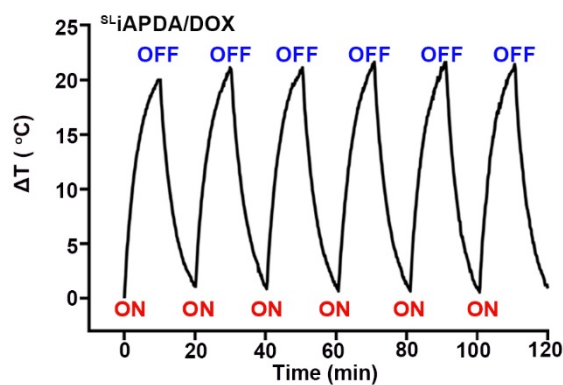


Fig. S8 Temperature changes of ^{SLi}iAPDA/DOX under 808 nm NIR irradiation (2 W/cm^2) for six cycles (10 min of irradiation for each cycle).

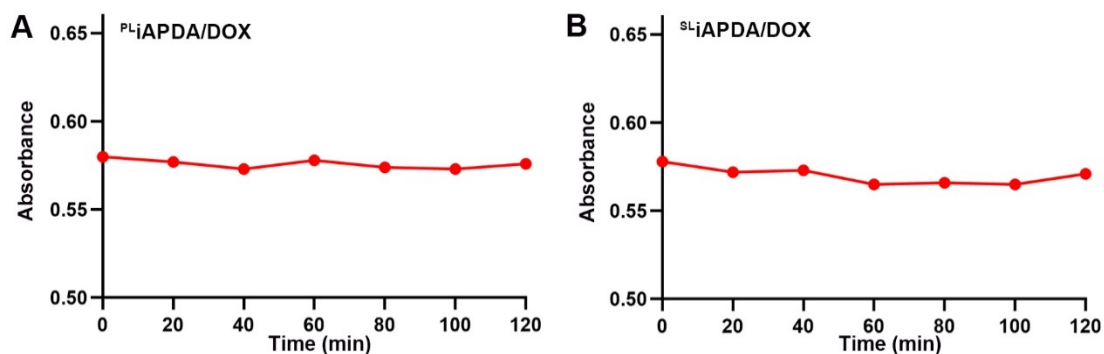


Fig. S9 Absorbance changes of ^{PLi}APDA/DOX (A) and ^{SLi}APDA/DOX (B) under 808 nm NIR irradiation (2 W/cm²) for six laser on/off cycles, respectively.

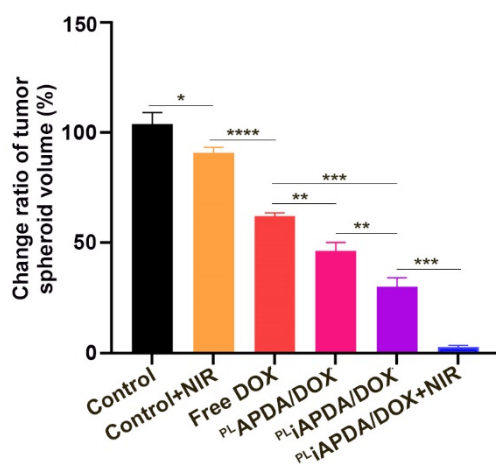


Fig. S10 Change ratios of 4T1 tumor spheroids volume (%) after applying various formulations and untreated control. Data were presented as mean \pm SD, $n = 5$; * $P < 0.05$, ** $P < 0.01$, *** $P < 0.001$, **** $P < 0.0001$.

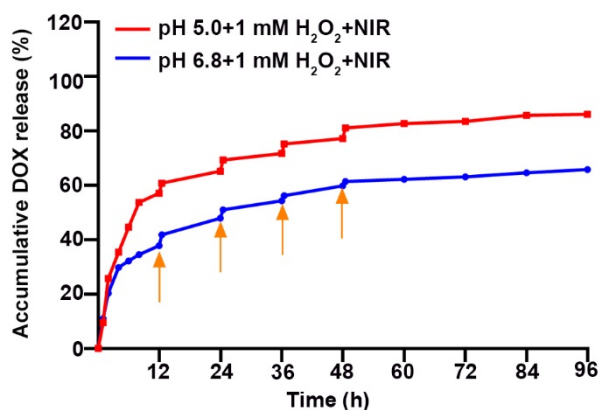


Fig. S11 Accumulative release of DOX from ^{PLi}APDA/DOX triggered by NIR irradiation (2 W/cm², 10 min), ROS (1 mM H₂O₂), and different pH values (5.0, 6.8) to

simulate the tumor microenvironment, respectively. Data were presented as mean \pm SD, $n = 3$.

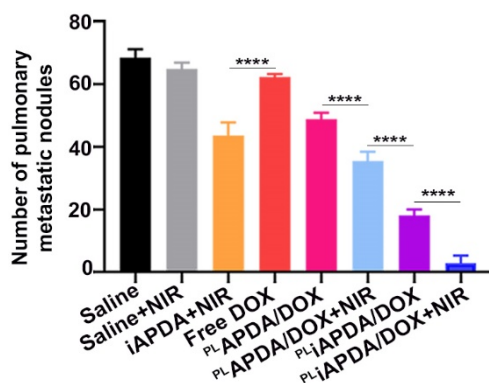


Fig. S12 Number of pulmonary metastatic nodules of 4T1 tumor-bearing mice after various treatments indicated. Data were presented as mean \pm SD, $n = 5$; **** $P < 0.0001$.

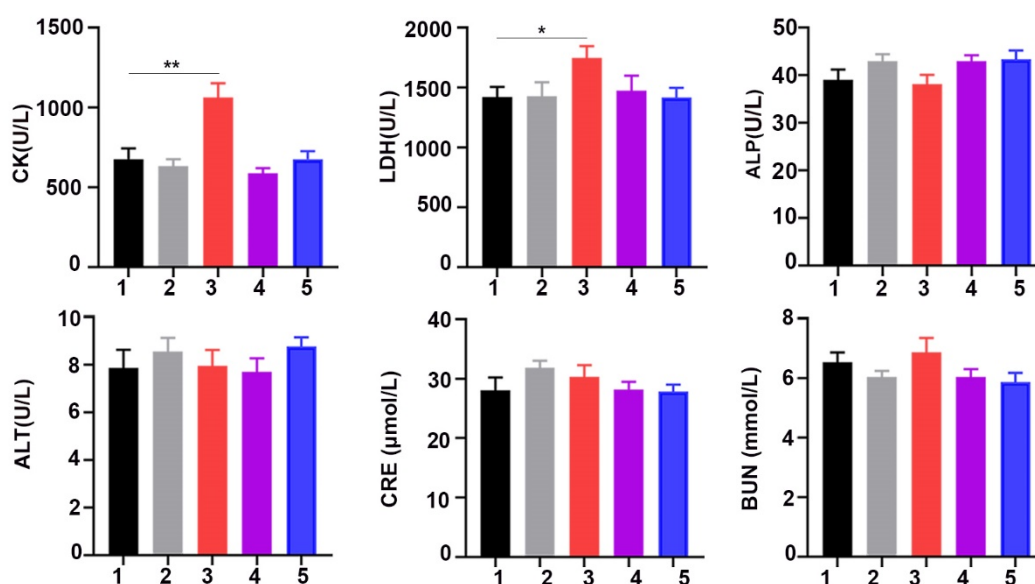


Fig. S13 Biochemical studies including heart functions (CK, LDH), liver functions (ALP, ALT), and renal functions (CRE, BUN) in healthy mice treated with various treatments (1, saline; 2, saline with irradiation; 3, free DOX; 4, ^{PLi}APDA/DOX; 5, ^{PLi}APDA/DOX with irradiation). Dose of DOX: 1.5 mg/kg; irradiation: 808 nm at 2 W/cm² for 10 min. Data were presented as mean \pm SD, $n = 5$; * $P < 0.05$. ** $P < 0.01$.

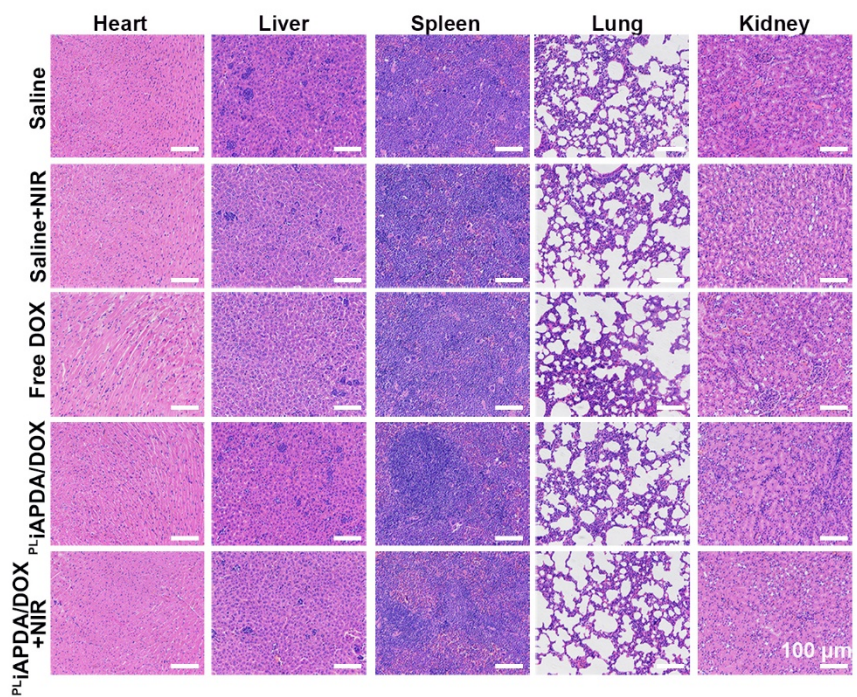


Fig. S14 H&E histopathological sections of tissues excised from mice in the study groups. Scale bar = 100 μm.

Table S1 Characterization of different formulations, including PDA, ^{PL}PDA/DOX, ^{SL}PDA/DOX, ^{PLi}APDA/DOX, and ^{SLi}APDA/DOX. Data were presented as mean \pm SD, $n = 3$.

	Diameter (nm)	PDI	Zeta potential (mV)	EE (%)	DL (%)
PDA	84.54 \pm 0.79	0.18 \pm 0.03	-21.05 \pm 0.60	---	---
^{PL} PDA/ DOX	107.70 \pm 2.73	0.25 \pm 0.01	16.20 \pm 1.08	79.71 \pm 2.29	70.51 \pm 0.59
^{SL} PDA/ DOX	105.32 \pm 2.14	0.15 \pm 0.04	7.92 \pm 1.01	24.39 \pm 3.13	42.23 \pm 1.11
^{PLi} APDA /DOX	123.80 \pm 1.87	0.19 \pm 0.04	-29.31 \pm 4.04	79.71 \pm 2.29	57.79 \pm 0.48
^{SLi} APDA /DOX	119.10 \pm 0.65	0.18 \pm 0.03	-35.17 \pm 6.02	24.39 \pm 3.13	34.91 \pm 0.91

Table S2 Grafting rate of iRGD-apoA-I to PDA nanoparticles in different formulations. Data were presented as mean \pm SD, $n = 3$.

Mass ratio (iA:PDA/DOX)	^{PLi} APDA/DOX	^{SLi} APDA/DOX
0.1:1	(8.49 \pm 0.27) %	(8.39 \pm 0.30) %
0.15:1	(12.28 \pm 0.15) %	(12.17 \pm 0.19) %
0.25:1	(18.03 \pm 0.27) %	(17.33 \pm 0.29) %
0.35:1	(18.26 \pm 0.31) %	(17.53 \pm 0.72) %

Table S3 IC₅₀ of iAPDA + NIR, Free DOX, ^{PL}APDA/DOX, ^{PL}APDA/DOX, ^{PL}iAPDA/DOX, and ^{PL}iAPDA/DOX + NIR.

	iAPDA +NIR	Free DOX	^{PL} APDA/ DOX	^{PL} iAPDA/ DOX	^{PL} iAPDA/DOX +NIR
IC ₅₀ (μg/mL)	46.68	1.53	1.28	0.95	0.61